Supporting Information

A Selectively Bimodal Flexible Sensor Based on IL/SWCNTs/PEDOT:PSS Nanocomposite for Material and Shape Recognition

Shen Yuan[1,2#], Yuchen Tian[1,2#], Yue Li[1,2#], Shengzhao Li[1,2], Lei Fu[1,4], Tie Li[1,2,3] and Ting Zhang[1,2]**

Yuan Shen, Yuchen Tian, Yue Li, Shengzhao Li, Lei Fu, Prof. T. Li, Prof. T. Zhang

[1]i-Lab Suzhou Institute of Nano-Tech and Nano-Bionics (SINANO)

Chinese Academy of Sciences (CAS)

398 Ruoshui Road, Suzhou 215123, P. R. China.

[2]School of Nano-Tech and Nano-Bionics, University of Science and Technology of China (USTC), Hefei, Anhui, 230026, P.R. China.

Prof. T. Li

[3]Jiangxi Institute of Nanotechnology

278 Luozhu Road, Xiaolan Economic and Technological Development Zone, Nanchang, 330200, China.

Lei Fu

[4]Gusu Laboratory for Materials Science

388 Ruoshui Road, Suzhou, 215123, P. R. China.

[#] These authors contributed equally to this work.

*Corresponding authors: tli2014@sinano.ac.cn (Tie Li), tzhang2009@sinano.ac.cn (Ting Zhang).

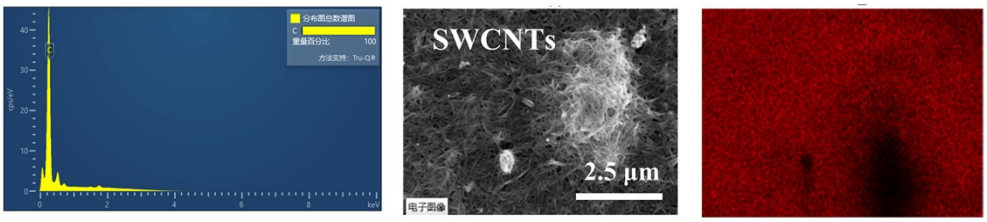

Figure S1. The energy dispersive X-ray spectroscopy (EDS) of SWCNTs.

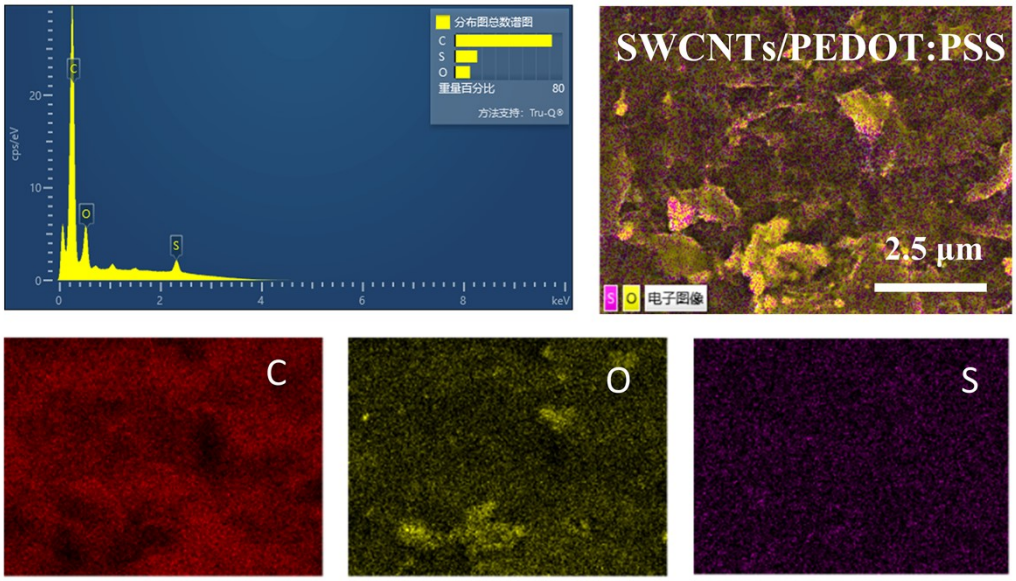

Figure S2. The EDS of the SWCNTs/PEDOT:PSS nanocomposite.

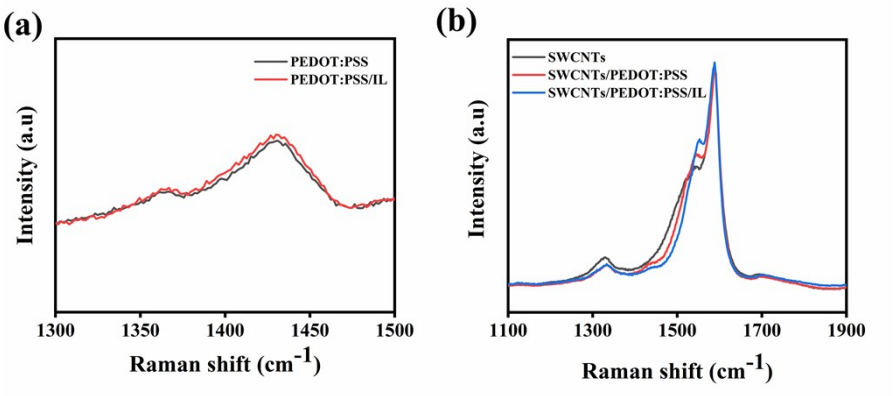

Figure S3. Enlarged Raman spectra of the nanocomposite with various compositions. (a) Spectra of the PEDOT:PSS and IL/PEDOT:PSS samples, where the content of IL is fixed at 75 wt%. (b) Spectra of the SWCNTs, SWCNTs/PEDOT:PSS, IL/SWCNTs/PEDOT:PSS samples, where the IL content and PEDOT:PSS content are fixed at 75 wt% and 70 wt%, respectively.

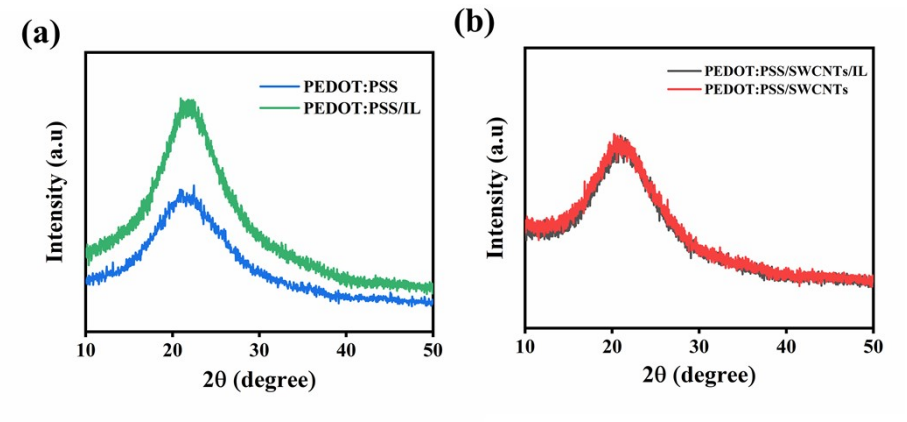

Figure S4. Enlarged X-ray diffraction (XRD) patterns of the nanocomposite with various compositions. (a) Spectra of the PEDOT:PSS and IL/PEDOT:PSS samples, where the content of IL is fixed at 75 wt%. (b) Spectra of the SWCNTs/PEDOT:PSS, IL/SWCNTs/PEDOT:PSS samples, where the IL content and PEDOT:PSS content are fixed at 75 wt% and 70 wt%, respectively.

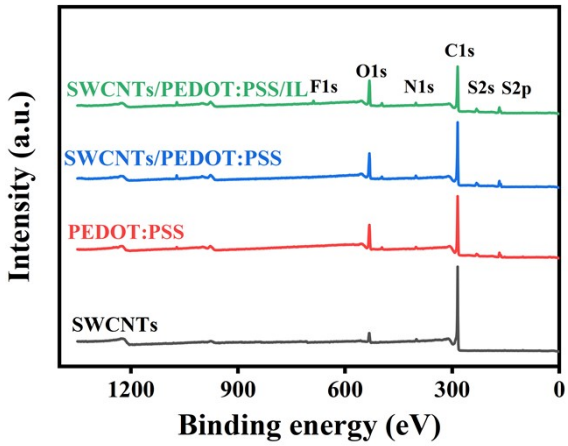

Figure S5. X-ray photoelectron spectroscopy (XPS) survey of the sensitive nanocomposites with various components.

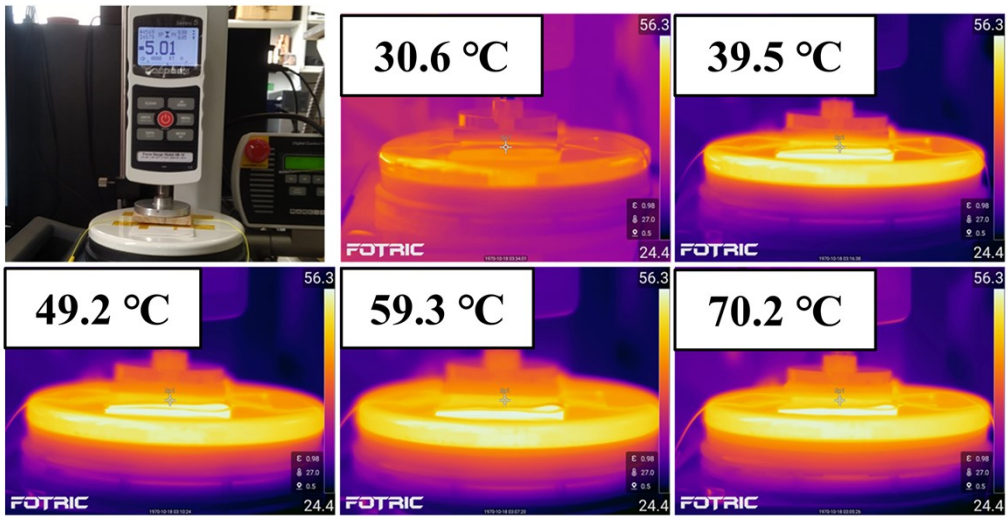

Figure S6. Thermal imaging photographs of the temperature and force dual-mode response behaviors of the flexible tactile sensor in the interference-free response test.

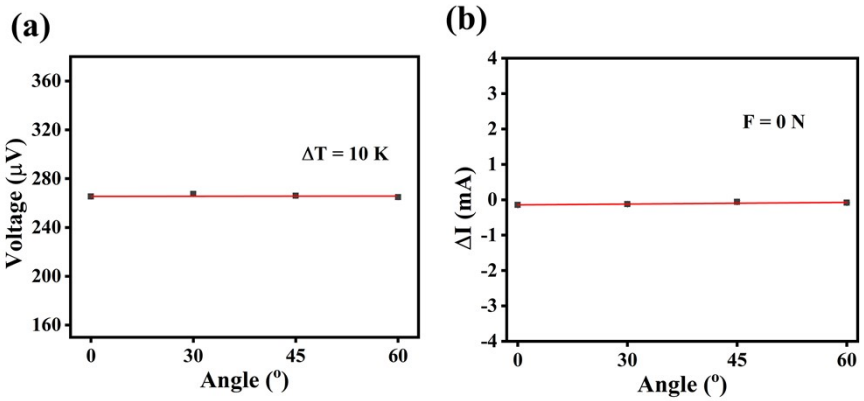

Figure S7. Temperature and force sensing properties of the flexible tactile sensor based on IL/SWCNTs/PEDOT:PSS nanocomposite film. (a) The output voltages of the sensor versus various bending angle. (i) The terminal current of the sensor versus bending angle.

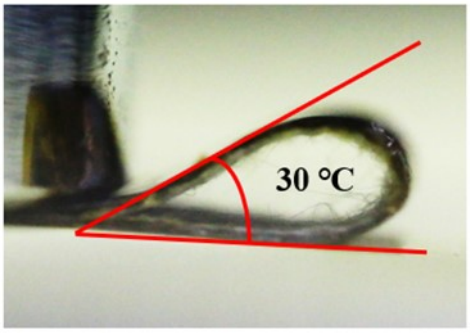

Figure S8. Photography and bending radius of the flexible sensor under extreme bending.

We have also measured the bending radius of the sensor, and the result displays that the sensor has the ability to bend up to 150°, which profits from the great flexibility of the sensitive material and the interdigital electrode.

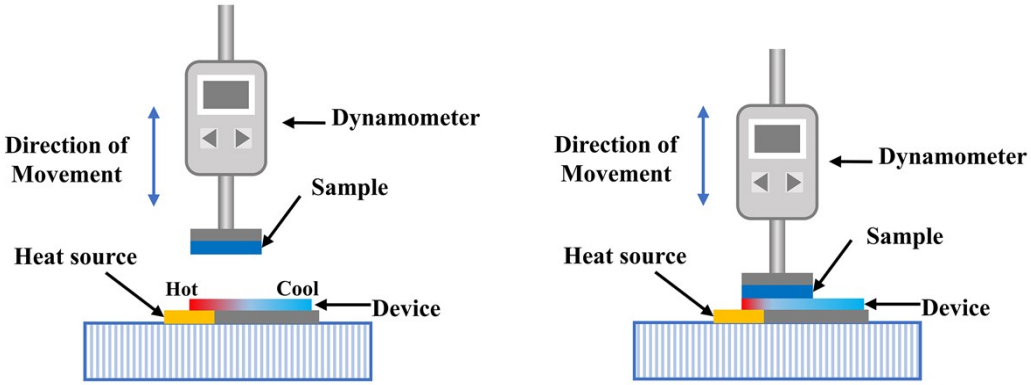

Figure S9. The schematic diagram of the test method for material identification.

Supplementary Table:

Table S1. The positions and peak width at half height of the characteristic peaks of the various controlled samples.

Sample	PEDOT:PSS	IL/ PEDOT:PSS	SWCNTs	SWCNTs/ PEDOT:PSS	IL/SWCNTs / PEDOT:PSS
Peak position / cm^{-1}	1430.92	1430.06	1588.24	1588.24	1588.24
Peak width at half height / cm^{-1}	72.84	74.37	48.41	46.43	41.91

Table S2. The peak width at half height of the various controlled samples.

Sample	PEDOT:PSS	IL/ PEDOT:PSS	SWCNTs/ PEDOT:PSS	IL/SWCNT/ PEDOT:PSS
Peak width at half height / cm^{-1}	13.09	12.61	15.64	13.09